Journal of Alloys and Compounds 509 (2011) 997–1000

Contents lists available at ScienceDirect

Journal of Alloys and Compounds

journal homepage: www.elsevier.com/locate/jallcom

Magnetic properties of Fe–Co–Mo–Cu–B nanocrystalline ribbons with stressing surfaces

Pavol Butvin*, Beata Butvinová, Peter Švec Sr., Gabriel Vlasák, Dušan Janičkovič

Institute of Physics, Slovak Academy of Sciences, 845 11 Bratislava, Slovak Republic

ARTICLE INFO

Article history:
Received 28 June 2010
Received in revised form 27 August 2010
Accepted 1 September 2010

Keywords:
Nanostructured materials
Rapid-solidification
Anisotropy
Magnetization
Magnetic measurements

ABSTRACT

Magnetic properties of Fe–Co–Mo–Cu–B alloy system with Co up to 26 at.% were investigated. After proper thermal treatment, the nanocrystalline grain remains tiny, the density hardly increases, but the room-temperature saturation attains 1.5 T mainly due to a high enough Curie temperature. The generally observed slant hysteresis loops point to ribbon surfaces, which stress the ribbon interior and induce a specific magnetoelastic contribution to hard-ribbon-axis magnetic anisotropy even after vacuum annealing. The effect does not come from cobalt but rather from the lack of silicon. Partial removal of the surfaces resulted in a decrease of the loop tilt.

1. Introduction

Diverse motivation stood behind an attempt to test the properties of Fe–Co–Mo–Cu–B alloy system. Compared to the proven Fe–Nb–Cu–B–Si (Finemet) composition, several potential improvements were targeted.

- Co is substituted for certain part of Fe to increase the magnetic saturation and possibly also the Curie temperature (the latter was already confirmed [1]). An extended temperature range for stable nanocrystalline structure can be achieved this way too.
- To use Mo instead of Nb for the role of grain stabilization is due to other reasons. Not only is Mo cheaper but Nb is temporarily labeled as "strategic" due to highly uneven occurrence of its source ores. However, Mo lowers the Curie temperature more than Nb.
- Alloying yet another element with such effect should possibly be avoided – silicon is thus not present. Moreover Si in Fe–Co based ribbons deteriorates soft-magnetic properties and appears to enable viscous flow at a moderate tension (few MPa) when the alloy is annealed. This flow is accompanied by significant, mostly undesired, magnetic anisotropy as reported recently [2]. Nevertheless, omitting silicon in the composition frequently results in vulnerable surfaces since no protective SiO_x surface layer is formed as shown for similar materials [3]. Moreover, corrosion studies show that even this protection diminishes when crystalline phase appears [4].

However, the diversity between the surfaces and the ribbon interior comes right from the planar-flow casting on air as already noted [5]. The impact of the diversity can be significant particularly on materials with a high surface/volume ratio – as shown by thin ribbons. Although a direct influence of annealing ambience cannot be excluded, the surface as-cast diversity does not disappear but inevitably transforms even during high-vacuum annealing when performing XPS [6]. We use the term macroscopic heterogeneity (MH) for all this surface-to-interior diversity. It frequently results in mutual in-plane stress between the surfaces and the interior. Fe–Co–Nb–B Hitperm is a good example of a positively magnetostrictive material, where surfaces squeeze the interior and create a significant hard-ribbon-axis magnetic anisotropy that tilts the hysteresis loops. Potting such a ribbon to a squeezing resin jacket demonstrates well, that the characteristic slant loop is mostly due to magnetoelastic interaction [7,8]. The effect of in-plane stress on the anisotropy closely resembles the situation in magnetostrictive films deposited on a substrate with different thermal expansion [9]. This contribution to anisotropy is not always detrimental for possible practical use. Anyway, it is a risk factor.

* Corresponding author at: Physics of Metals, Institute of Physics, Slovak Academy of Sciences, Dúbravská cesta 9, 845 11 Bratislava, Slovak Republic.
Tel.: +421 2 5941 0560; fax: +421 2 5477 6085.
E-mail address: fyzipbut@savba.sk (P. Butvin).

0925-8388/$ – see front matter © 2010 Elsevier B.V. All rights reserved.
doi:10.1016/j.jallcom.2010.09.154

Table 1
Sample identification and measured parameters.

Composition of ribbons	Label Co_x [at.%]	ρ as-cast [g/cm^3]	λ_s 540 °C vac [ppm]	H_{cd} 540 °C Ar [A/m]	H_{cd} 540 °C vac [A/m]	J_s 540 °C vac [T]
$Fe_{79}Mo_8Cu_1B_{12}$	Co_0	7.96	1.3	45	28	1.14
$(Fe_{12}Co_1)_{79}Mo_8Cu_1B_{12}$	Co_6	8.00	10.3	70	22	1.30
$(Fe_9Co_1)_{79}Mo_8Cu_1B_{12}$	Co_8	8.00	13.0	59	19	1.36
$(Fe_6Co_1)_{79}Mo_8Cu_1B_{12}$	Co_{11}	8.03	7.8	72	21	1.42
$(Fe_3Co_1)_{79}Mo_8Cu_1B_{12}$	Co_{20}	8.10	22.6	107	70	1.50
$(Fe_2Co_1)_{79}Mo_8Cu_1B_{12}$	Co_{26}	8.10	26.0	174	134	>1.40

Density ρ was measured on as-cast samples. Coefficient of saturation magnetostriction λ_s, dynamic (21 Hz) coercivity H_{cd} and room-temperature magnetic polarization at 2 kA/m J_s were determined after the indicated 1-h treatment. Co_{26} does not saturate at 2 kA/m.

2. Material and methods

The substitution of Co for Fe extends from $x=0$ to $x=26$ at.% in the $Fe_{79-x}Co_xMo_8Cu_1B_{12}$ composition. To inspect the effect of the lacking silicon, we tested also Si-containing $Fe_{73.5}Mo_3Cu_1B_9Si_{13.5}$ as a reference. The ribbons were prepared on air by planar-flow casting technique giving width of 6 mm and thickness of ~0.019 mm. Two annealing environments were used – vacuum (<10E−3 Pa) and technical purity Ar at atmospheric pressure. This is the simplest test to reveal MH as demonstrated [10]. Annealing temperatures were chosen above the primary and far below the second-stage crystallization temperatures according to DSC and thermogravimetry data already published [1]. Very fine (~5 nm) crystalline grain is generally observed after such a treatment [1,11] and there is no substantial difference between particular compositions. To remove surface layers, certain samples were etched in HF acid based lye. After determining the density of samples by buoyancy method, hysteresis loops were recorded on ribbon pieces at 21 Hz, sine H excitation along the ribbon long axis. The Helmholtz-coil based setup with two pick-up coils (only one is loaded by sample) is wired so, that not induction B but magnetic polarization J is obtained from the induced voltage sum. Proper demagnetization factor D was computed from the sample dimensions using elliptic integrals. Thus the internal field H_i was computed from the exciting current according to $H_i = H_{ext} - DJ/\mu_0$ (standard symbol meanings). Despite small sample volume, the density gives an accuracy of ±0.5%. The sample thickness was not directly measured but computed as the effective one with the use of sample length, width, mass and density. Magnetostriction was measured on circular discs with the help of a three-terminal capacitance method, which determines the changes of sample dimensions due to magnetic field.

3. Results and discussion

According to our experience, the low-frequency hysteresis loops are the universal means to resolve and characterize the difference between similar soft-magnetic materials as well as the changes due to various thermal treatments. The loops of as-cast precursor ribbons for a nanocrystalline material are the exception to the rule – they are quite alike and saturate poorly.

Moreover, the unprocessed ribbons frequently show a characteristic as-cast anisotropy which also emerges as an anisotropy of thermal expansion; it usually disappears after keeping the sample several minutes above 400 °C as shown for similar ribbons [12]. Despite the poor saturation, the difference to loops of annealed nanocrystalline samples (see Fig. 1) clearly shows how the magnetic anisotropy changed and the saturation increased due to stress transformation and T_C (Curie temperature) rise, respectively (see Table 1 for numeric values). At room temperature, the basic Co-free as-cast alloy Co_0 is above its T_C [1] and shows no hysteresis loop.

3.1. Changes due to vacuum annealing

First – all the loops after annealing are tilted as seen in Fig. 1. This applies to the complete Fe–Co–Mo–Cu–B alloy system irrespective of annealing ambience. The Co-free alloy is a reference to show, that cobalt does not appear to be the reason for the universal tilt. The tilt (together with variably pronounced central "belly") is a consequence of MH. It causes a hard-ribbon-axis (HRA) magnetic anisotropy of magnetoelastic origin and the major easy direction is pushed off the ribbon plane [7]. Molybdenum is hardly to be suspected although Pavuk et al. observed [13] that it does not stay away from crystalline grain as meticulously as niobium. The tilt itself shows no systematic correlation to any grain property (size, composition). Then, the lack of silicon must be the main culprit. Indeed, if the Si-rich Fe–Mo–Cu–B–$Si_{13.5}$ alloy is inspected (see Fig. 2), it shows the upright loop with essentially no HRA anisotropy even after Ar-annealing. Another point is to be made on the lacking silicon: the density increase due to annealing is reduced. Unlike the Si-rich comparable alloys, where this increase surpasses 2%, the increase in Fe–Co–Mo–Cu–B alloys hardly attains 0.5%, what is the resolution of our method. The vicinity to the resolution threshold could be the cause that no correlation of the density increase to Co percentage showed up clearly. However, the Co percentage emerges in another characteristic. If Co_{20} is compared to Co_6 (Fig. 1 and Table 1), it is seen, that not the loop tilt but the coercivity is larger and the loop acquires one more "knee" after annealing at the higher temperature. Such a behavior is often met when a new magnetic phase appears. At the time, we have no indication for a new phase - other than bcc Fe–Co as reported by Conde et al. [1]. Though it has been pointed out for very similar alloy system that Co promotes the crystallization of Fe borides [14], none were identified after an annealing below 600 °C. Thus we can suggest the observed Co-enrichment of the grains [11,14] as a preliminary

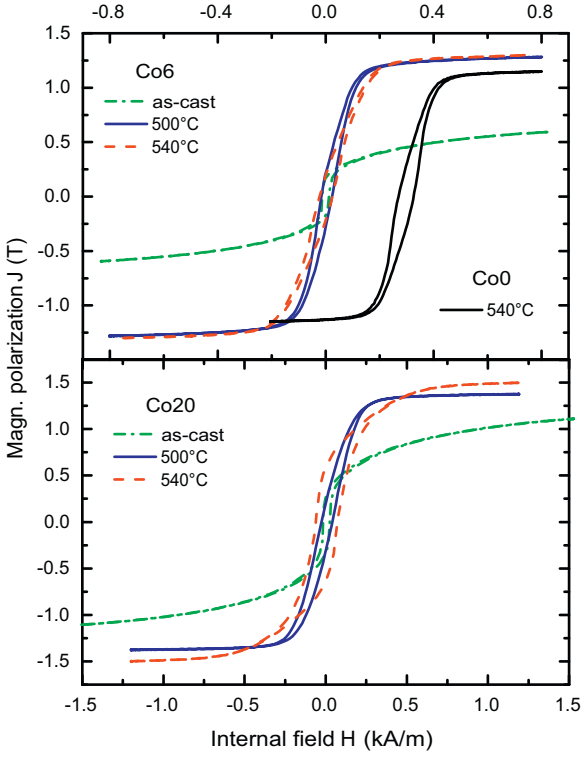

Fig. 1. Hysteresis loops showing the changes inferred by vacuum annealing – 1 h at the indicated temperature. Note that the loop for Co-free basic alloy is tilted too (it is plotted with +300 A/m shift to be discernible).

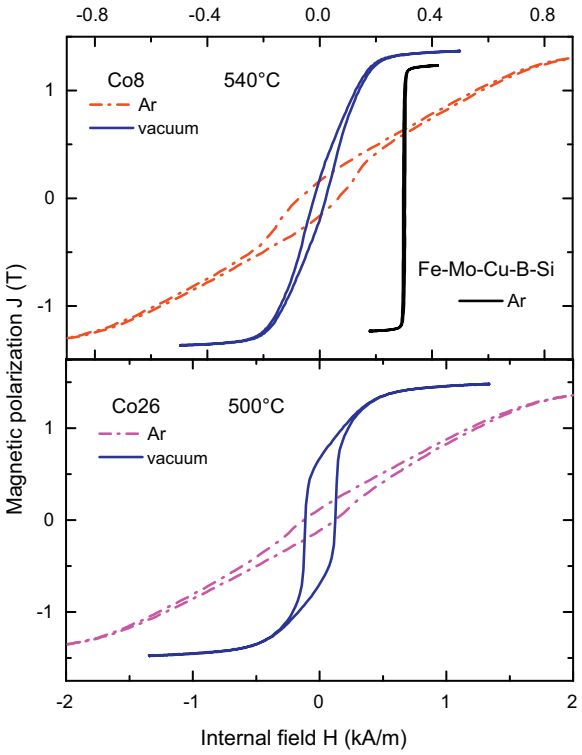

Fig. 2. Hysteresis loops of ribbons annealed for 1 h at different temperature and in different ambience. The reference ribbon (the loop is plotted shifted by 300 A/m) shows no impact of MH.

explanation for the magnetic hardening, which rather diminishes the loop tilt.

3.2. Differences due to annealing ambience

The huge difference of the loop tilt between vacuum and Ar annealed samples seen in Fig. 2 is a benchmark of MH influence. Not only is the annealing ambience chemically diverse, the different pressure influences the transformation of MH as well. Moreover, the density does not increase after Ar annealing. It rather decreases albeit within the limits of the density measurement resolution. The crystallization-induced density increase could point to a source of compressive stress exerted by surfaces on the ribbon interior. This is when crystallization is marked by increased density and is more advanced at the surfaces (e.g. surface crystallization). Apparently, this is not the case with these Fe–Co–Mo–Cu–B ribbons and the reason why the surfaces create the compressive in-plane stress is more complicated. The correlation of MH-induced anisotropy to magnetostriction is reflected too – larger tilt is observed for Co_{26}, which shows twice the magnetostriction of Co_8 (see Table 1). The comparison of Figs. 1 and 2 (the Co-free alloys) suggests that a "basic" loop tilt comes from the lack of Si. The strongly hysteretic part of the loop at small fields ("belly") is recognized to be a consequence of stripe domains switching by Hubert and Schäfer [15]. The prevalent reason for the occurrence of such domains is ascribed [15] to a perpendicular magnetic anisotropy with the easy direction pointing off the ribbon plane – as is the case of MH-influenced Fe–Co–Mo–Cu–B ribbons. Whereas this MH caused anisotropy appears to be the major reason for the central "belly" in Co_8, still another effect participates in Co_{26} (and Co_{20} after 540 °C annealing – Fig. 1). The strongly hysteretic part is namely too high in J to represent the domains dwelling in surface region only. The tilt of this part of the loop (vacuum annealing) is also significantly smaller. Thus, another effect takes over in the Co-rich alloys, which show the higher coercivity,

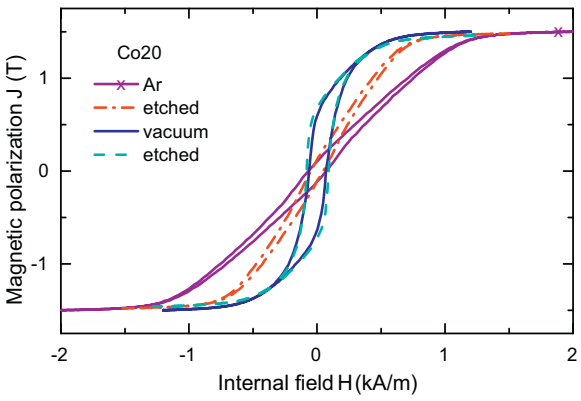

Fig. 3. Hysteresis loops of samples before and after etching. Ar annealing was performed at 500 °C for 1 h, whereas vacuum annealing was at 540 °C/1 h.

and only the significantly stronger MH after Ar annealing can be a match capable of tilting the whole loop. We thus retain the already mentioned Co enrichment [11] to account for the higher coercivity of Co_{20} and Co_{26} (see also Table 1).

3.3. Changes due to surface removal

We chose to ablate the ribbon surfaces by etching Co_{20} samples the same time in the same lye despite of the different sample annealing. It was instructive to observe that whereas the thickness reduction of the Ar annealed sample attained 8%, it was just the half (4%) for the vacuum annealed sample. Thus, the surfaces after different annealing are inherently different. We chose the higher vacuum annealing temperature intentionally to see whether MH is resolvable even on the sample, where it represents the minor effect, which influences the loop. Indeed, the effect of surface removal is minute and is not well seen in Fig. 3. Thus, we enhanced the resolution by using the so-called magnetization work W (after Chikazumi [16]), which is closely related to anisotropy energy and is easily computed from a digitized loop. The HRA anisotropy (as induced by MH) is well reflected by the magnetization work. It actually decreases even due to minor surface removal from the vacuum annealed sample – from 238 to 210 J/m^3. The Ar annealed sample shows substantially larger effect – the HRA anisotropy is reduced almost by half showing W falling from 810 to 485 J/m^3. The larger thickness reduction is for sure not the major reason for the Ar-annealed sample to show such an enhanced W reduction. To compute always the correct sample cross section, we checked precisely the changes of all the sample dimensions and the weight change caused by etching. The minor difference in (technical) saturation could be due to a tiny average density increase after surface removal. If so, the loops after etching would show even slightly smaller W – i.e. still larger etching effect. We also checked the surface morphology by microscope. No discernible systematic changes due to the etching were resolved. Thus the most straightforward explanation of the surface removal effect is the reduction of the in-plane compressive stress (squeeze) which the MH influenced surfaces exert on the ribbon interior. It follows then, that Ar annealing creates far stronger stress than vacuum annealing.

If certain parameters (coercivity, core loss, saturation) could be accepted, one can exploit the slant loop for a specific purpose – e.g. for a no-slit choke core. Co_{11} provides the best parameters from this viewpoint. It shows 1.39 T saturation, 15 A/m dynamic coercivity and 79 J/m^3 magnetization work after 1-h 500 °C vacuum annealing (see Fig. 4).

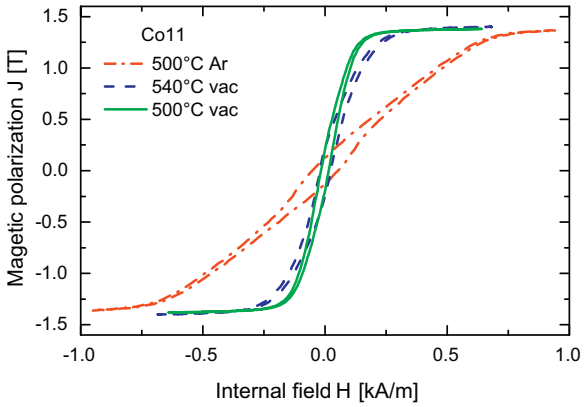

Fig. 4. Hysteresis loops of Co_{11} showing the best soft-magnetic properties after 500 °C annealing in vacuum. Duration of each annealing was 1 h.

4. Conclusion

The Fe–Co–Mo–Cu–B alloy system represents one of the alternatives to Finemets or Hitperms in the quest for an improved soft-magnetic material. It appears that mainly the lack of silicon and too much cobalt impose the limits to the soft-magnetic properties at least within the investigated composition range. The macroscopic heterogeneity restricts the possibility to tailor the magnetic anisotropy and magnetic softness goes lost with high Co percentage. However, acceptable properties can be achieved by choosing the right composition (∼11 at.% Co) and optimizing the thermal treatment.

Acknowledgments

This work was supported in part by the national grant agencies VEGA under grants No 2/0156/08; 2/0157/8 and APVV under grant No 0413-06. The authors are also grateful to Centrum of Excellence “Nanosmart” for additional support.

References

[1] C.F. Conde, A. Conde, D. Janičkovič, P. Švec, J. Magn. Magn. Mater. 304 (2006) e739.
[2] B. Butvinová, P. Butvin, G. Vlasák, P. Švec, D. Janičkovič, Rev. Adv. Mater. Sci. 18 (2008) 509.
[3] J.E. May, C.A.C. Souza, C.L. Morelli, N.A. Mariano, S.E. Kuri, J. Alloys Compd. 390 (2005) 106.
[4] A.K. Panda, M. Manimaran, S. Basu, A. Mitra, I. Chattoraj, J. Mater. Sci. 40 (2005) 4579.
[5] R. Jain, N.S. Saxena, K.V.R. Rao, D.K. Avasthi, K. Asokan, S.K. Sharma, Mater. Sci. Eng. A297 (2001) 105.
[6] S.P. Chenakin, G.G. Galstyan, A.B. Tolstogouzov, N. Kruse, Surf. Interface Anal. 41 (2009) 231.
[7] P. Butvin, B. Butvinová, J. Sitek, J. Degmová, G. Vlasák, P. Švec, D. Janičkovič, J. Magn. Magn. Mater. 320 (2008) 1133.
[8] K. Hayashi, M. Hayakawa, Y. Ochiai, H. Matsuda, W. Ishikawa, K. Aso, J. Appl. Phys. 55 (1984) 3028.
[9] K. Yamada, A. Fujita, M. Ohta, K. Fukamichi, J. Magn. Magn. Mater. 239 (2002) 412.
[10] B. Butvinová, P. Butvin, R. Schäfer, Sens. Actuators A 106 (2003) 52.
[11] C.F. Conde, A. Conde, Rev. Adv. Mater. Sci. 18 (2008) 565.
[12] P. Butvin, B. Butvinová, G. Vlasák, P. Duhaj, M. Chromčíková, M. Liška, E. Illeková, P. Švec, J. Phys.: Conf. Ser. 144 (2009) 012101.
[13] M. Pavúk, M. Miglierini, M. Vujtek, M. Mashlan, R. Zboril, Y. Jirásková, J. Phys.: Conf. Ser. 19 (2007) 216219.
[14] J. Torrens-Serra, P. Bruna, S. Roth, J. Rodriguez-Viejo, M.T. Clavaguera-Mora, J. Alloys Compd. 496 (2010) 202.
[15] A. Hubert, R. Schäfer, Magnetic Domains: The Analysis of Magnetic Microstructures, Springer-Verlag, Berlin, 1998, p. 478.
[16] S. Chikazumi, Physics of Magnetism, Wiley, New York, 1964, pp. 17, 263.